

Comprehensive Risk Assessment of Carbon Nanotubes Used for Agricultural Applications

Sajedeh Rezaei Cherati, Muhammad Anas, Shijie Liu, Sudha Shanmugam, Kamal Pandey, Steven Angtuaco, Randal Shelton, Aida N. Khalfaoui, Savenka V. Alena, Erin Porter, Todd Fite, Huaixuan Cao, Micah J. Green, Alexei G. Basnakian, and Mariya V. Khodakovskaya*



Cite This: *ACS Nano* 2022, 16, 12061–12072



Read Online

ACCESS |

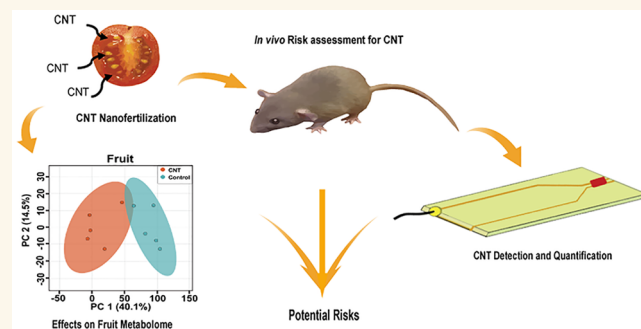
Metrics & More

Article Recommendations

Supporting Information

ABSTRACT: Carbon-based nanomaterials (CBNs) are often used for potential agricultural applications. Since CBNs applied to plants can easily enter plant organs and reach the human diet, the consequences of the introduction of CBNs into the food chain need to be investigated. We created a platform for a comprehensive investigation of the possible health risks of multiwalled carbon nanotubes (CNTs) accumulated in the organs of exposed tomato plants. Quantification and visualization of CNTs absorbed by plant organs were determined by microwave-induced heating (MIH) and radio frequency (RF) heating methods. Feeding mice with CNT-contaminated tomatoes showed an absence of toxicity for all assessed animal organs. The amount of CNTs accumulated inside the organs of mice fed with CNT-containing fruits was assessed by an RF heating technique and was found to be negligible. Our work provides the experimental evidence that the amount of CNTs accumulated in plant organs as a result of nanofertilization is not sufficient to induce toxicity in mice.

KEYWORDS: Carbon-based nanomaterials, nanofertilization, toxicity, plant metabolomics, risk assessment



The discovery of nanosized materials represented the beginning of a new and exciting scientific era, including applications in agriculture and the food industry.^{1–4} The application of nanomaterials can provide solutions for enhancement of plant productivity through the direct application of nanomaterials to plants known as nanofertilization, delivery of a wide range of compounds to plant cells using nanomaterials as carriers, or use of nanoparticles as nanosensors.^{5,6} Carbon-based nanomaterials (CBNs) have been described as one of the most promising classes of man-made nanomaterials suggested for agricultural applications.⁵ Thus, the use of CBNs in crop management techniques can offer an innovative approach for the improvement of plant growth and stress tolerance. A wide range of CBNs (single-walled and multi-walled carbon nanotubes, graphene, and nanohorns), added in low doses to seeds or growth medium (hydroponics, soil, water spray), can significantly activate germination, growth, flower/fruit production, and stress tolerance in food and nonfood plant species.^{7–14} The penetration ability of CBNs was utilized in the development of technologies focused on the delivery of chemicals and nucleic acids into plant cells using CBNs as carriers. Demirer et al. demonstrated the ability of carbon nanotubes (CNTs) to efficiently deliver DNA to plant cells

and emphasized the great potential of CBNs in plant improvement through genetic engineering.¹⁵ CBNs can be effectively used in biochemical sensing *in planta*. Giraldo et al. described the ability of single-walled carbon nanotubes (SWCNT) to sense nitric oxide in extracted chloroplasts and leaves.¹⁶ This discovery demonstrates the potential of CBNs for the detection of a wide range of molecules as well as chemical compounds in plant cells.^{16,17} It is known that carbon-based nanoparticles can be absorbed by exposed seeds and plants and thus move into different organs, including fruits.^{7,9,11} These findings indicate that the use of CBNs as delivery carriers, sensors, or growth regulators will lead to “nano-contamination” of exposed plants and the possible introduction of CBNs into the food chain. A comprehensive assessment of the risks associated with the toxicity of CBN-exposed plant organs (leaves, roots, fruits, and seeds) to

Received: March 3, 2022

Accepted: July 19, 2022

Published: July 22, 2022



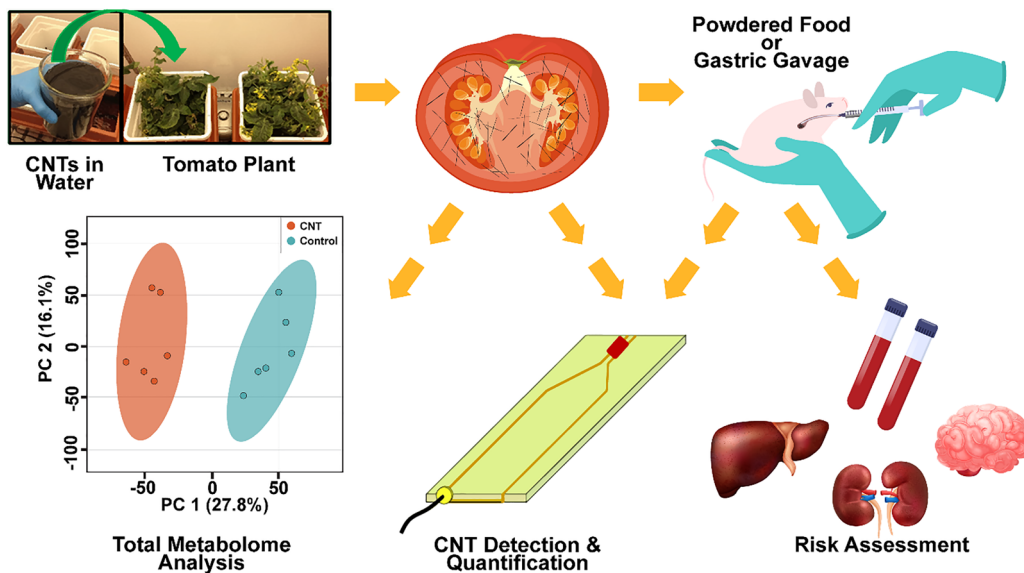


Figure 1. Experimental platform for complex *in vivo* risk assessment of CNT-containing plant organs after consumption as diet components. At the end of the cultivation period, organs of tomato plants exposed to a hydroponic solution supplemented with CNT were used for the detection of CNT using microwave-induced heating (MIH) and radio frequency (RF) heating methods. Fruits from CNT-treated and control plants were used for the analysis of total metabolome and *in vivo* studies involving the mouse model.

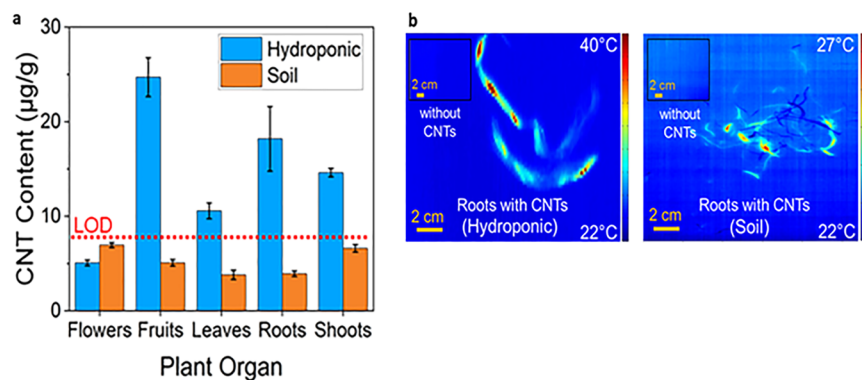


Figure 2. Quantification and visualization of CNT uptake by tomato plants grown in hydroponics or soil supplemented with CNTs. (a) Average CNT amount absorbed by organs of tomato plants cultivated in hydroponic solution and soil supplemented with CNTs was measured using the MIH method. (The calibration curve presented in Figure S1 relates MIH behavior with the CNT content, with a LOD (limit of detection) of 8 $\mu\text{g/g}$.) Error bars represent SE ($n = 6$). (b) RF heating imaging of the presence of CNTs inside of roots exposed to CNTs through the hydroponic solution and CNT-supplemented soil. Thermal maps of tomato roots, both with and without CNTs added to the cultivation system, were obtained after scanning the samples through a 72 MHz, 50 W RF field at a rate of 0.56 cm/s (schematic of the RF technique is shown in Figure S2).

potential consumers is critical for the approval of nanotechnologies for the agricultural industry. The efficiency of such an assessment depends on the creation of appropriate platforms for toxicological studies (*in vitro* and *in vivo*) and the establishment of highly sensitive methods for accurate quantification of nanomaterials absorbed by exposed plants and transferred to organs of consumers (animals, humans). The toxicity of plant organs contaminated with nanomaterials can arise from two sources: directly from absorbed CNTs, or from increases in the production of potentially toxic plant metabolites caused by CNTs. Both types of potential toxicity should be carefully evaluated in risk assessment studies.

Here, we developed a platform for a comprehensive assessment of the risks associated with the utilization of agricultural plants contaminated with nanomaterials through the use of nanoparticles as sensors, growth regulators, carriers of biomolecules, and nanoparticles delivered to plants from

contaminated soils (Figure 1), typically in the form of powders or dispersions. The key task is the ability to make direct links between the amount of absorbed CNTs by plants, the potential toxicity of contaminated plant organs, and the amount of CNTs accumulated inside animal organs as a result of CNT-containing fruit consumption. To achieve this, we utilized a method for quantification of CNTs inside animal and plant organs based on electromagnetic heating. Combined with the assessment of *in vivo* toxicity, this comprehensive approach allowed us to estimate the potential risks of the inclusion of CNT-contaminated plants into the food chain.

RESULTS AND DISCUSSION

Quantification of CNTs Inside Organs of Tomato Plants. To measure the accumulation of CNTs inside plant organs, we determined the exact amount of CNTs absorbed by tomato organs after cultivation of plants in a hydroponic

solution supplemented with CNTs (100 mg/L) for 10 weeks and after cultivation of plants in CNT-supplemented soil (60 mg/400 g of soil or 150 mg/kg; Figure 2). It is important to note that any possible interference from the organic matter in the soil is accounted for because the control samples would have the same organic matter present. The doses of CNTs selected for plant cultivation have been previously described as the most effective concentrations of CNTs for plant growth regulation.¹⁸ Quantification of absorbed CNTs was performed using the Microwave Induced Heating; (MIH) method.¹⁹ Figure S1 provides the calibration curve relating temperature change with the CNT content after 10 s of heating at 30 W and 2.45 GHz.

In this experiment, we determined that the amount of absorbed CNTs is linked to the specific method of CNT exposure. The experiment with CNTs in hydroponic solution led to higher CNT accumulation inside fruits, shoots, leaves, and roots of exposed tomato plants as compared to the experiments with a soil mix (delivery of CNT solution to the soil). The difference in CNT absorption may occur because CNTs are more mobile in an aqueous environment as compared to the soil mix, allowing for higher CNT uptake of the hydroponics-grown plants. The highest amount of CNTs was found in the roots and fruits of plants grown in CNT-supplemented hydroponics as compared to all other plant organs in both CNT-supplemented soil and CNT-supplemented hydroponics (Figure 2). RF heating has proven to be a reliable method to indicate the presence of other types of nanomaterials (graphene, carbon black, etc.) previously in various other substances.^{11,19,20} The RF heating method was used to provide thermal images of roots that were directly exposed to CNT solution. This method yields relative CNT distribution and displays hotspots in specific organs.²¹ CNTs in the sample rapidly heat up in response to RF fringing fields, unlike the unresponsive baseline matrix, and the heat signature from the CNTs is measured using a thermal camera. Figure S2 provides a schematic of the experimental setup of RF imaging of plant organs. Thermal mapping of roots (Figure 2b; Figure S3) demonstrated significantly more heating in the roots of hydroponically grown plants compared to roots of soil-grown plants, suggesting a higher CNT content in hydroponics samples, which is consistent with the data in Figure 2a.

Analysis of Total Metabolome in Various Organs of CNT-Exposed Tomato Plants. It is known that carbon-based nanomaterials can affect the molecular level of plants and influence the overall plant transcriptome and certain metabolic pathways.^{7,18} We aimed to understand if CNTs absorbed by plants can significantly affect the total metabolome of organs directly soaked in solution supplemented with CNTs (roots) and organs without direct contact with the CNT solution (stem, leaves, flowers, fruits). To do so, we analyzed the total metabolome of all organs of tomato plants grown in CNT-supplemented hydroponics using liquid chromatography–mass spectrometry (LC-MS; Figure 3; Table S1, Figure S4). Principle component analysis (PCA) proved that CNTs significantly affected the tomato metabolome in all analyzed organs (Figure 3). Expression of 1293, 214, 408, 368, and 260 metabolites identified by KEGG (Kyoto Encyclopedia of Genes and Genomes) in roots, stems, leaves, flowers, and fruits, respectively, were significantly either upregulated or downregulated in response to CNT application (Table S1). A portion of differently regulated metabolites can be associated with metabolic pathways using KEGG metabolic pathway

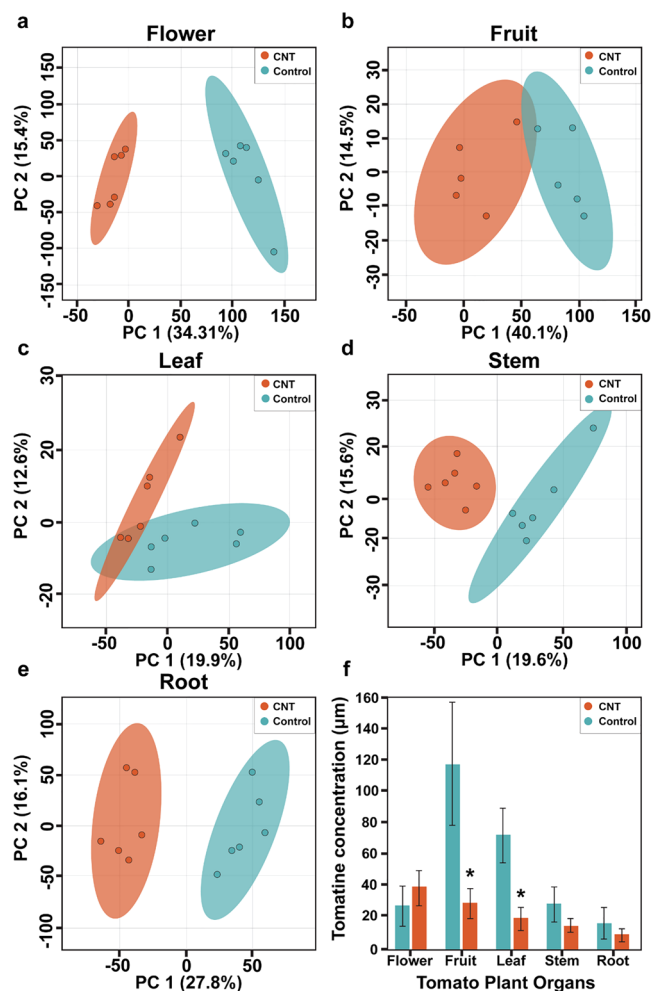


Figure 3. Visualization of metabolomics differences of tomato organs collected from unexposed tomato plants and plants exposed to hydroponic solution supplemented with CNTs. (a–e) Principal component analysis (PCA) comparing total metabolome of CNT-exposed (CNTs) with unexposed (control) tomato plants using MetaboAnalyst. Each dot represents an individual sample, red for CNTs and green for control ($n = 6$). Surrounding clouds are the 95% confidence intervals. (f) Tomatine concentration in CNT-exposed and unexposed (control) tomato plant organs. One-sample T-test was done on tomatine sample concentrations ($*p < 0.05$).

enrichment analysis (Figure S5). CNT-affected metabolic pathways were conserved in all analyzed tomato organs and associated with six major metabolic pathways: biosynthesis of secondary metabolites, carbon metabolism, ATP-binding cassette (ABC) transporters, an amino sugar and nucleotide sugar metabolism, and biosynthesis of amino acids (Figure S5). A list of all dysregulated metabolites in five analyzed tomato organs and pathways associated with CNT-affected metabolites are shown in Tables S2–S11. Observed modifications in secondary metabolism caused by CNTs can potentially lead to elevation of toxic plant metabolite concentrations. However, analysis of CNT-affected metabolites identified by LC-MS (Tables S2–S11) did not identify up-regulated metabolites with potential toxicity to humans. To confirm this conclusion, we analyzed the production of the potentially toxic metabolite tomatine, a steroid glycoalkaloid that is produced by tomato and potato organs (Figure 3f). It is reported that tomatine can

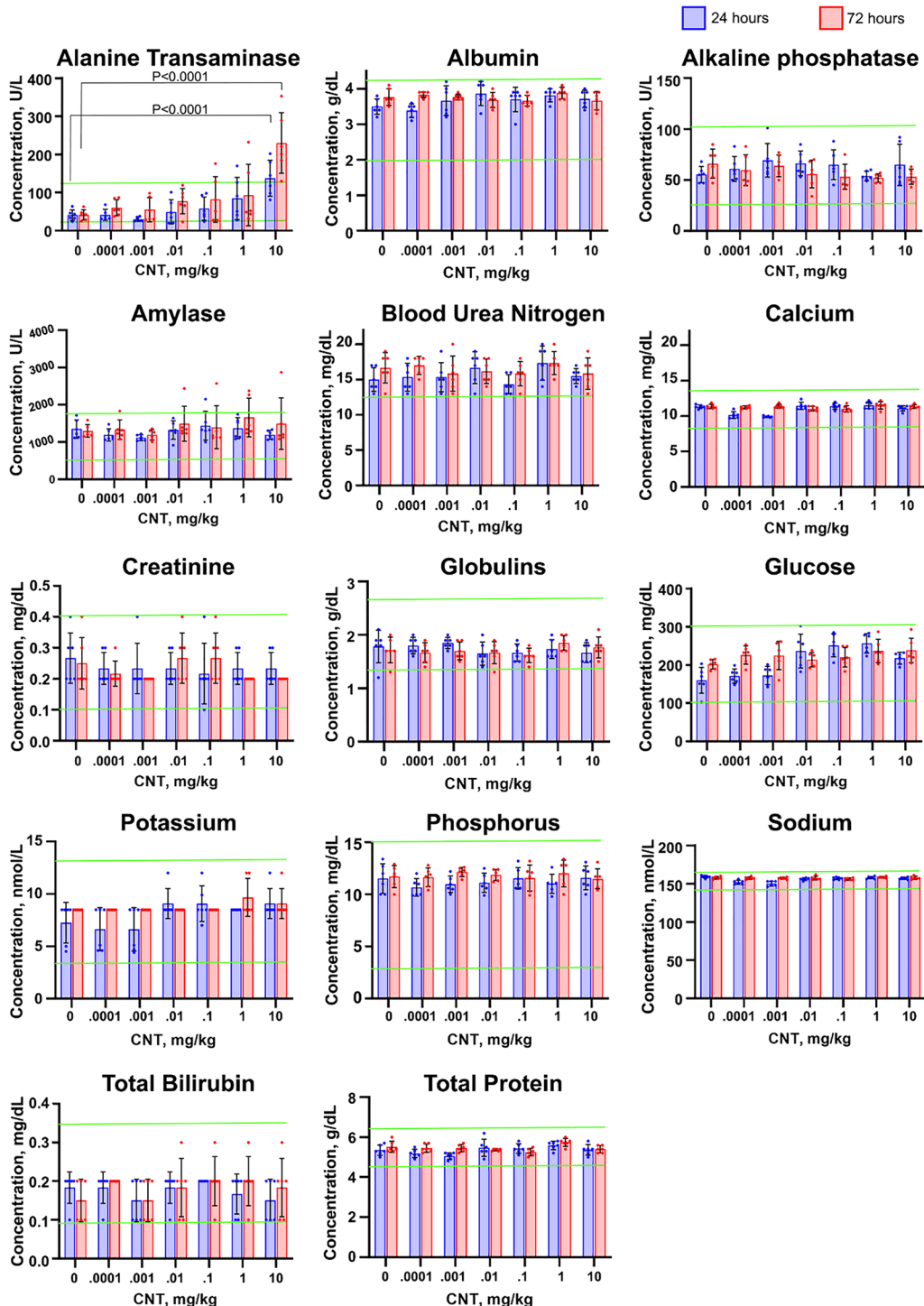


Figure 4. Measurements of 14 markers of various organ functions for the assessment of functional toxicity of CNTs given to mice by gastric gavage 24 or 72 h after a single dose between 0 and 10 mg/kg ($n = 6$; mean \pm SD, p values are shown in the graph). Normal ranges for the blood marker are shown by light green lines. Only one marker of liver toxicity, alanine transaminase (ALT), is significantly elevated above the zero control and beyond the maximal normal level.

protect tomato plants against biotic stress imposed on plants due to antifungal and anti-insecticidal properties.²² Although regular ripe tomatoes are producing tomatine at nonharmful concentrations, there are reports about various side effects of tomatine at higher concentrations. For example, at high doses, tomatine may form a nonabsorbable complex with cholesterol and other sterols in the enteral lumen, which may affect the absorption of cholesterol.²³ We found that exposure of tomato

plants to CNTs added to the hydroponics system did not induce the production of tomatine in any analyzed organs but instead reduced the amount of this metabolite in fruits and leaves (Figure 3f).

Thus, we can conclude that absorbed CNTs significantly affected the total metabolome in all organs of exposed tomato plants. However, this modification did not result in the upregulation of known toxic compounds in tomatoes. It is

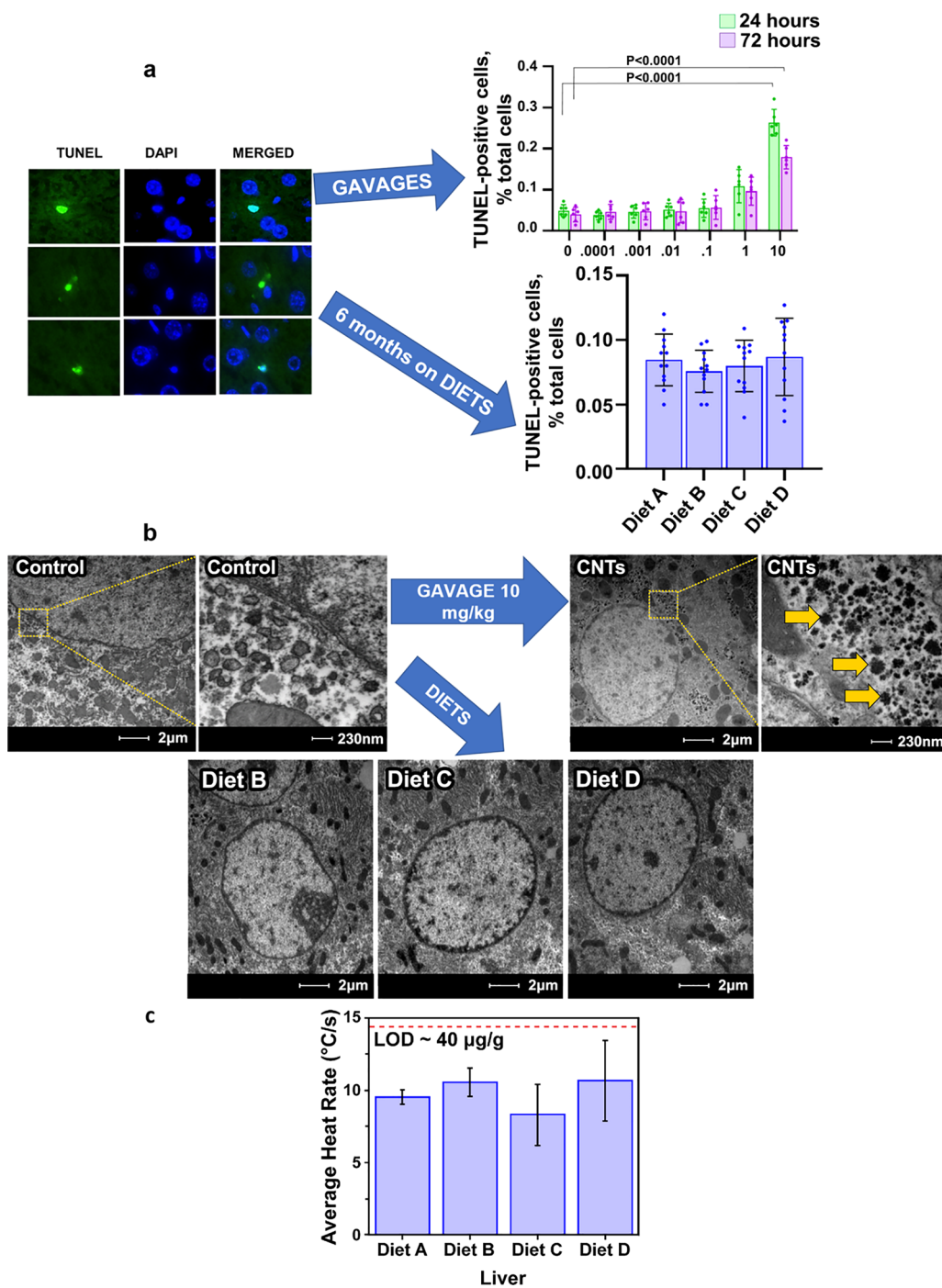


Figure 5. Assessment of structural changes within the liver associated with the presence of CNTs in the liver of mice exposed to pure CNTs (gavage) or tomato fruits contaminated with CNTs (diets). (a) Assessment of structural injury to the liver of mice exposed to pure CNTs (gavage) or CNT-contaminated fruits (diets) using TUNEL assay. Diet A = mice fed with powdered regular mouse chow (PRMC); diet B = mice fed with 95% PRMC + 5% dried control tomato fruit powder (TFP); diet C = mice fed with 95% PRMC + 5% control TFP and added pure CNTs (25 μ g/g); diet D = mice fed with 95% PRMC + 5% CNT-grown TFP. The TUNEL assay performed on liver sections 24 or 72 h after CNT gavages at doses from 0 to 10 mg/kg showed significant elevation of DNA fragmentation (% TUNEL-positive, dead cells; $n = 6$; mean \pm SD) at a dose of 10 mg/kg. There was no statistically significant difference observed between the diets in the TUNEL assay 6 months after the start of the diets ($n = 12$; mean \pm SD). (b) TEM of liver cells of mice exposed to pure CNTs (gavage) or CNT-contaminated fruits (diets). The presence of dense CNT granules in hepatocytes (shown by yellow arrows) was observed in the liver 72 h after CNT gavage (10 mg/kg). TEM did not reveal any inclusions in hepatocytes of mice fed with diets. (c) Estimation of the amount of CNTs accumulated in the liver cells of mice fed with CNT-containing diets by determination of average heat rate using an RF heating method. The calibration curve relating heat rate with the CNT content in the liver is shown in Figure S7. The heating was induced using an RF (138 MHz) power of 20 W, and the heating rate was calculated for an initial \sim 1 s of heating. LOD is 40 μ g/g. The statistical differences between diets were not significant as determined by comparisons of diets C and D to diet B ($p > 0.05$).

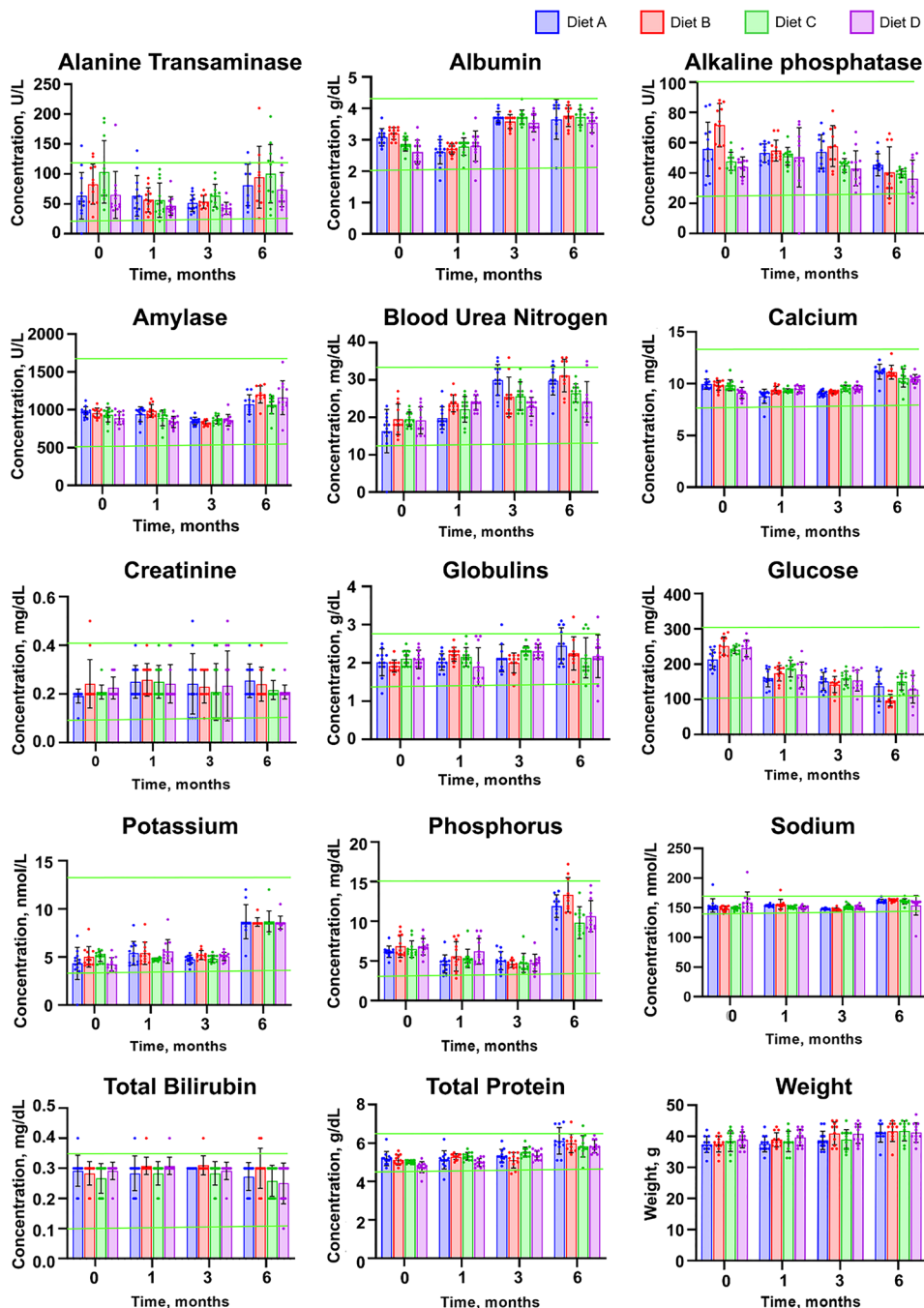


Figure 6. Assessment of toxicity of tomato fruits contaminated with CNTs in mice. Mice were fed with four diets, and organs' functions were assessed at 0 point and 1, 3, and 6 months after the start of the diets by measuring 14 blood plasma markers ($n = 12$; mean \pm SD; p values are shown in the graph). Normal ranges for the blood marker are shown by light green lines. Diet A = mice fed with powdered regular mouse chow (PRMC); diet B = mice fed with 95% PRMC + 5% dried control tomato fruit powder (TFP); diet C = mice fed with 95% PRM + 5% control TFP and added pure CNTs (25 μ g/g); diet D = mice fed with 95% PRMC + 5% CNT-grown TFP.

unlikely that CNT-induced changes in tomato metabolism can contribute to the possible toxicity of tomato organs containing CNTs. To investigate the potential toxicity of fruits collected from CNT-exposed tomato plants, we performed prolonged *in vivo* experiments using mice.

Analysis of Toxicity of CNT-Containing Tomato Fruits in a Mouse Model. Toxicity assessment of CNT-containing fruits was initiated from the determination of the doses of pure CNTs that can cause toxicity in mice. For this study, CNTs in a wide range of doses (0.001; 0.01; 0.1; 1; 10 mg/kg) were administered to mice in water suspensions via oral gavage

(Figure 1). To monitor the function of organs after CNT exposure, 14 parameters of the comprehensive diagnostic profile—including alanine aminotransferase, albumin, alkaline phosphatase, amylase, blood urea nitrogen, calcium, creatinine, globulin, glucose, phosphorus, potassium, sodium, total bilirubin, and total protein—were analyzed in blood to quantitatively assess functions of the liver, kidney, heart, intestine, pancreas, and other organs that could be affected by the CNTs (Figure 4). The terminal deoxynucleotidyl transferase dUTP nick-end labeling (TUNEL) assay, the most sensitive and universal assay for irreversible cell death,^{24,25} was

used for assessment of the structural toxicity of the nanoparticles (cell death). Our data indicated that a single oral gavage of CNTs induced only moderate liver injury and only at the highest tested dose (10 mg/kg), as evident by an elevation of a sensitive liver toxicity marker, serum alanine transaminase (ALT; *Figure 4*). The TUNEL assay also confirmed liver damage at a CNTs dose of 10 mg/kg (*Figure 5a*). All 13 other organ function markers did not demonstrate any significant difference from the control sample (water gavage; *Figure 4*). Because the determined concentration of CNTs in tomato fruits is several times less than the 10 mg/kg shown in *Figure 2a*, the data indicate that the CNT concentrations found in tomato fruits are likely to be nontoxic to animals.

We were able to visualize CNTs delivered at the highest tested dose (10 mg/kg) in liver tissue by using dark-field microscopy (DFM) and transmission electron microscopy (TEM). We found that DFM did allow the quantification of nanoparticle aggregates due to the low sensitivity of DFM at the CNT concentration observed in the liver. Our data showed that some DF-positive objects (particles) were observed in both TUNEL-positive (dead) and TUNEL-negative (alive) liver cells even without CNT feeding, indicating that mice got some particulate matter from regular chow without CNTs (*Figure S6*). Importantly, CNT gavage induced an overall elevation of DF-positive objects (most likely CNT aggregates), in both dead and alive liver cells. Dead cells contained more particles in both CNT-fed animals and the control group. TEM was more accurate and allowed the confirmation of the presence of CNTs inside cells of the livers of mice who received a dose of CNTs (10 mg/kg) associated with observed toxicity in blood experiments (*Figure 4*, *Figure 5a*). It was found that the nanoparticles that looked like corpuscular objects (CNTs) were accumulated inside some hepatocytes, and these cells remained alive (*Figure 5b*). This is an indication that some mouse's liver cells are capable of accumulating CNTs without inducing immediate cell death.

In the second *in vivo* experiment, the toxicity of fruits collected from CNT-exposed tomato plants was assessed (*Figure S8*). Periodic feeding of mice with dried CNT-containing tomato fruits was performed for 6 months. The experiment was started with 48 CD-1 male mice, which were divided into four groups: diet A (mice fed with powdered regular mouse chow (PRMC)), diet B (mice fed with 95% PRMC + 5% dried control tomato fruit powder (TFP)), diet C (mice fed with 95% PRM + 5% control TFP and added pure CNTs in concentration that was the same as the amount of CNTs in fruits collected from hydroponically grown tomato plants (25 μ g/g)), and diet D (mice fed with 95% PRMC + 5% CNT-grown TFP). During six months of *in vivo* study, each mouse on diet D got approximately 1.82 mg of CNTs arriving from contaminated fruits. Quantification of nanomaterials accumulated by organs of orally exposed animals is a challenging task.²⁶ However, the determination of the absorbed amount is critical for the establishment of the link between applied nanomaterial and its potential toxicity. Microscopical and spectroscopic methods of detection of nanomaterials allow the visualization of nanoparticles in organs²⁷ but do not provide quantifications of nanomaterials accumulated in organs. Here, we applied the RF heating method for quantification of CNT amounts in organs of animals that consumed CNT-contaminated fruits. Dried mice organs were collected at the end of the experiment, ground,

and analyzed by RF heating (*Figure S9*). *Figure 5c* demonstrates average heat rates for livers from mice fed with control diets (A, B) and CNT-containing diets (C, D). The differences between the CNT-containing diets and control diets were not significant, and the CNT contents corresponding to the heat rates were below the detectable threshold associated with our calibration (*Figure S7*). Similar findings were obtained for other organs such as the brain and kidney (*Figure S10*). The potential toxicity of all diets (A–D) was assessed by several methods. First, the toxicity of CNT-containing fruits was assessed with blood tests. Blood was collected to monitor toxicity at the baseline, as well as at 1 month, 3 months, and 6 months of feeding, and subjected to the 14 organ function assays. As shown in *Figure 6*, all tested blood markers, including ALT, were within normal ranges for diets C and D and did not reveal any statistical difference compared to the controls (diets A and B) at all time points (*Figure 6*). TUNEL confirmed the absence of structural damage in the liver (*Figure 5a*), and TEM images of livers collected from animals that received diets C and D were similar to the control and had no CNT visual inclusions (*Figure 5b*). While information about the dietary toxicity of pure CNTs in mammals is limited, studies have shown that CNTs can accumulate in animal organs and produce toxic effects if administered intravenously,²⁷ inhaled,²⁸ or applied on the skin.²⁹ Several studies were focused on the determination of the distribution of CNTs via the oral route.³⁰ In one study, 3 h after oral administration, labeled CNTs were found in all 12 analyzed organs of animals.³¹ Cell and tissue injury caused by CNTs was associated with free radical generation, oxidative stress, inflammation, and apoptosis.^{29,32,33} Fortunately, the majority of CNTs are excreted through biliary and renal pathways, and even their accumulation in tissues over 3 months does not necessarily lead to toxicity.²⁷ For example, an early study that aimed to determine the potential toxicity of CNTs in mice using histology and Raman microscopic mapping demonstrated that the CNTs persisted within liver and spleen macrophages for several months without apparent toxicity.³⁴ The level of toxicity of CNTs is strictly related to applied concentration. Thus, the oral uptake of CNTs in high concentrations (10 and 50 mg/kg) led to reproductive system injury and sperm toxicity in male mice.³⁵ Here, we confirmed that a high dose of CNTs (10 mg/kg) administrated orally can lead to liver damage. However, working with tomato fruits contaminated with CNTs as a result of the use of CNTs as plant growth regulators, we did not observe any measurable accumulation of CNTs in the liver, brain, and kidney and did not detect toxicity associated with the changes in fruit metabolomes caused by CNTs or CNTs consumed with CNT-contaminated tomato fruits. Our experiments provide evidence that the low amount of CNTs accumulated in tomato fruits (25 μ g/g of dry fruit) as a result of nanofertilization is insufficient to cause toxicity during prolonged oral administration of CNT-contaminated fruits. Significantly higher amounts of CNTs are linked with the accumulation of CNTs in animal organs and toxicity to cells. Results established by *in vivo* studies are in a good correlation with our previous *in vitro* experiments involving tomato fruits contaminated with CNTs as a result of nanofertilization.³⁶ This early study demonstrated that the concentration of CNTs accumulated in contaminated tomato fruits was not sufficient to have an effect on the total gene expression of human intestinal epithelial cells (T-84) and change the transepithelial

resistance of T-84 cells. Additionally, extracts from CNT-contaminated fruits did not affect human intestinal microbiota as was evident by 16S rRNA sequencing.³⁶

CONCLUSIONS

CBNs already play a critical role in increasing plant productivity and food security in challenging climate conditions. Different plant products were developed with the help of CBNs used as growth regulators, sensors, and carriers of chemicals/nucleic acids or applied in food packaging. The safety of such products must be demonstrated before adding new technologies to the market. The establishment of links between the amount of nanoparticles absorbed by exposed plants and potential toxicity to animals and humans has been limited by the lack of quantitative methods permitting the assessment of CBNs inside plant and animal organs. Using advanced methods of quantification of CBNs in biological samples (MIH, RF heating), we were able to link the amount of CNTs absorbed by plant organs (tomato fruits) with the amount of CNTs accumulated in organs of animals (mice) which were consuming CNT-containing fruits. Combined with the assessment of *in vivo* toxicity, this comprehensive detection approach allowed us to evaluate the potential risks of the inclusion of CNT-contaminated plants into the food chain. On the basis of the data, we concluded that there is no measurable accumulation of CNTs in organs (liver, kidney, brain) of mice fed with CNT-contaminated tomato fruits, and there is no detectable toxicity associated with the tomato fruits grown in the presence of CNTs used as growth regulators. The study establishes a platform for the assessment of risks associated with nanomaterials entering into the food chain. These results suggest that the potential use of carbon-based nanomaterials as nanofertilizers would pose low risks to consumers of agricultural plants.

MATERIALS AND METHODS

Preparation of Nanomaterials. Multi-walled CNT-COOH (OD 13–18 nm; length 1–12 μm) were obtained from US Research Nanomaterials, Inc. (Houston, TX). Characterization of used CNTs by transmission electron microscopy (TEM) and thermal gravimetric analysis (TGA) was performed as described previously.⁹ The potential contaminant, endotoxin, was removed from the CNTs by three constitutive rounds of autoclavation as described by Lahiani et al.³⁷ CNTs were sonicated before use. The probe sonicator Qsonica with 500 W of power and a 20 kHz frequency was used for sonication of CNT suspension. One liter of 1 g/L CNT suspension was sonicated for 30 min in a 5-s, 3-s pulse with 70% amplitude.

Cultivation of Plants in the Presence of Nanomaterials. Exposure of tomato plants to CNTs was performed by cultivating them in a hydroponic system supplemented with the CNTs or soil supplemented with CNTs dispersed by ultrasound prior to use. Both the control plants and the plants exposed to CNTs, for both hydroponics and the soil experiment, were grown at the University of Arkansas in Little Rock (UALR) in a controlled environmental facility (greenhouse) under an 8-h light (26 °C)/16-h dark (22 °C) cycle. Plants were grown under the conditions of 45% humidity and 500 $\mu\text{mol}/\text{m}^2/\text{s}$ light. The hydroponic system was obtained from Hydrofarm (Grand Prairie, TX). An air pump system was linked to the hydroponic system to keep roots and nutrient solutions well aerated. A water pump was used to provide a continuous flow of the nutrients and CNTs. The trays were filled with 10 L of deionized water and supplemented with 0.5 mL of nutrient solution per 1 L of water. GENERAL HYDROPONICS FloraNova growth solution was used as the nutrition solution for the hydroponics system. CNTs were added to the seedlings in hydroponics to the final concentration of

100 $\mu\text{g}/\text{mL}$ for three consecutive weeks. Plants were grown in hydroponics for 10 weeks, and ampules were collected for the metabolomics study and detection of CNT inside tomato organs. For the experiment involving CNT exposure in soil, 3-week-old tomato seedlings were transferred to the soil and grown in a greenhouse. A 100 mL solution of CNT suspension (200 $\mu\text{g}/\text{mL}$) was added to 4-week-old tomato plants once a week for three consecutive weeks in each experimental pot containing 400 g of soil. The final amount of CNTs in each pot was 60 mg per 400 g of soil. For control (untreated) plants, 100 mL of deionized water was applied at the same time. An equal amount of pure water was used for regular irrigation of control and CNT-treated plants daily. Samples of different organs were collected from 16-week-old plants. Sungro HORTICULTURE growing mix was used for the soil experiment. The behavior of added CNT in the hydroponics solution and water mix used for addition to soil was analyzed by measurement of dynamic light scattering, zeta potential, and absorbance (Table S12).

Quantification of the Amounts of Absorbed CNTs in Organs of Exposed Plants. We used our previously developed method to determine CNT content in plant organs of hydroponically and soil-grown plants.^{14,18} The method, as described by Irin et al. in 2012, quantitatively detects CNT content through a calorimetry analog, where the CNT loading is correlated with temperature rise (ΔT) due to absorption of microwave power.¹⁹ A calibration curve is made by creating samples with known amounts of CNTs (ng) per milligram of sample, and a linear relationship is found between CNT (ng) per milligram of sample and temperature rise. The samples with an unknown amount of CNTs are then measured, and a temperature difference is recorded. The calibration curve is used to work backward to find the amount of CNTs (ng) per mg of sample based on the unknown samples' temperature difference. The animal samples measured have a weight that ranged from 10 to 20 mg. The plant samples had a weight that ranged from 100 to 200 mg. Prior to microwave (2.45 GHz) exposure in a custom waveguide, the samples were powdered using a mortar and pestle and dried under a vacuum at 50 °C to remove moisture. During microwave exposure, the temperature rise was measured using a K-type thermocouple. A calibration curve relating temperature change and CNT content (after 30 W, 10 s exposure) is provided in Figure S1. The intercept is calculated using the response of the control sample for each organ. A CNT content per mass of any sample ($\mu\text{g}/\text{g}$ sample) was determined by comparing the temperature rise of the sample to the established calibration curve (Figure S1).

Radio Frequency (RF) Thermal Mapping of Plant Organs. A fringing-field capacitor with two parallel 30-cm-long copper tracks spaced 5 mm apart was fabricated to couple RF fields with plant organs. As-received whole plant organs were scanned over the capacitor with a 72 MHz 50 W RF field at a speed of 0.56 cm/s. A forward-looking infrared (FLIR) camera was used to monitor the heating response (Figure S3), and thermal maps were generated by analyzing FLIR data using MATLAB. Note that the samples had to be flat to allow for uniform heating and reliable imaging. Organs such as fruits and shoots are problematic in this regard, so it was quite difficult to map CNT distribution in these organs.

Analysis of Total Plant Metabolome by LC-MS. Tomato flowers, green and red fruits, leaves, stems, and roots were collected and snap-frozen in liquid nitrogen. Samples were collected from plants exposed to CNT and the control. Tomato samples were stored at –80 °C for further sample extraction. Frozen tomato organs of CNT-exposed and control samples were powdered in the presence of liquid nitrogen in a mortar and pestle. From the initial 40 mg of plant tissue, approximately 20 mg was powdered and transferred to Eppendorf tubes. The powdered tissue was extracted using 80% HPLC-grade methanol for each of six biological replicates. The samples were subsequently vortexed (1 min), sonicated (15 min), and centrifuged for 5 min at 10 000 rpm. The supernatants were filtered into microcentrifuge tubes through 25 mm, 0.2 μm syringe filters. The tubes were dried overnight in a 45 °C vacufuge, and the dried samples were stored at –80 °C the next day. Samples were reconstituted to equal volume using 80% HPLC-grade methanol and again vortexed,

sonicated, and centrifuged. The supernatants were filtered and transferred to autosampler vials and analyzed immediately. Leaves, stems, roots, and fruits were collected from fully mature tomato plants grown in the hydroponics system and used for LC-MS analysis. Fruit, leaf, root, and stem samples from control plants and CNT-treated tomato plants were analyzed using a Hichrom C-18 (Hichrom Expert in Chromatography, UK) reverse phase column on a Thermo Scientific UltiMate 3000 series HPLC (Thermo Scientific, Germering, Germany) equipped with an LPG-3400SD pump, WPS-3000 autosampler, TCC-3000 column oven, DAD-3000 diode array detector, and LTQ XL mass spectrometer system. The aqueous phase was acidified HPLC-grade water (0.05% formic acid (A)), and the organic phase was HPLC-grade methanol (B). Ten microliter injections were pumped at 0.6 mL/min with the following elution gradient: 0–6 min, 5% B; 6–14 min, 60% B; 14–38 min, 80% B; 38–38.5 min, 5% B; 38.5–40 min. The detection of tomato metabolites was performed by negative-mode electrospray ionization in a trap-mass spectrometer scanning 110–2000 *m/z*. The target was set at 10 000 and the maximum accumulation time at 30.00 ms with two averages. Xcalibur software (Xcalibur Software - Thermo Fisher Scientific) provided with the LCMS instrument was used to analyze samples and collect data. Files were loaded into MZmine software (<http://mzmine.github.io/>) and processed as was described by Pluskal et al.³⁸ The KEGG database was used for tentative online compound identification, which was completed through MZmine using the gap-filled peak list.³⁹ Further statistical analysis was carried out by uploading the identified peak list to Metaboanalyst (<http://www.metaboanalyst.ca/>) for analysis and by comparing it with data from available literature sources.⁴⁰

HPLC of Tomatine. A reverse-phase high-performance liquid chromatograph equipped with a mass spectrometer was used for analyzing the toxic compounds. The samples were extracted with 80% HPLC-grade methanol. Analysis of LC-MS was performed on a C18 column in a linear gradient system using two mobile phases, acidified water with 0.05% formic acid, and acetonitrile. A mixed serial dilution of tomatine was prepared in a range of 5–500 μ M. LC-MS analysis was performed for all standards where 10 μ L injections were pumped at 0.4 mL/min with the following elution gradient: 0–0.25 min, 20% B; 0.25–17 min, 100% B; 17–17.1 min, 5% B; 17.1–20 min. After analysis of data in MZmine, peak area and retention time were recorded for each component. A calibration curve was plotted of the peak area vs concentration using Excel. The calibration curves were represented by linear equations of $Y = 6353X + 80065$ for the tomatine standard. LC-MS was performed on plant samples of all organs with 100 μ M tomatine as the internal standard. Peak area and retention time were obtained after analysis of data in MZmine and the use of a calibration curve to determine the concentration of each component in the samples.

In Vivo Studies. All animal experiments were performed at the Central Arkansas Veterans Healthcare System (John L. McClellan Memorial Veterans Hospital in Little Rock, AR) and have been approved by the Institutional Animal Care and Use Committee. Male CD-1 mice (8 weeks old, 32–37 g) were purchased from Charles River Laboratories (Wilmington, MA) and fed with regular mouse chow before the experiment. We first tested the potential toxicity of pure CNTs. This direct exposure was necessary to establish that our methods allow the detection of CNT toxicity and that CNT toxicity actually exists. Without this experiment, any observed absence of toxicity could be interpreted as a false-negative result. A single dose of pure CNT suspended in water (\sim 0.2 mL) was administered orally by gastric gavage. The following experimental groups received CNT as a single dose in a range of concentrations: (1) 0 mg/kg (water control); (2) 0.001 mg/kg; (3) 0.01 mg/kg; (4) 0.1 mg/kg; (5) 1 mg/kg; and (6) 10 mg/kg. Twelve mice were used per group. Six of the animals in each group were euthanized 24 h after dosing, and six mice were euthanized 72 h after dosing. Blood and the following tissues were harvested: liver, kidney, spleen, lung, heart, aorta, intestine, pancreas, brain, bladder, skeletal muscle, skin, subcutaneous adipose tissue, and bone. Tissues were fixed in 10% buffered formalin and processed to determine CNT distribution. Blood was processed into serum, and

then blood chemistry markers were measured to determine organ toxicity. In total, 72 mice were used in this protocol. In the second tomato-feeding experiment, tomatoes containing CNTs and control CNT-free tomatoes were lyophilized, ground into a powder, and then mixed with a regular mouse chow powder feed at 5% tomato. There was also one group containing pure CNTs mixed with the powdered mouse food at a concentration of 25 μ g/g of tomato fruit powder. This group mimicked the real concentration of CNTs in hydroponic-grown tomato fruits measured by the MIH method as shown in Figure 2a. Once all of the food was mixed at the correct concentrations, it was mixed with 1% agarose as a personnel safety precaution to avoid unwanted distribution of the CNTs in the air. Experimental mice were fed *ad libitum* with mouse chow containing 5% dried tomatoes in groups, and one control group got only powdered mouse chow. Our goal was to study the potential toxicity of CNT-grown tomatoes at a level that is not lower than normal human consumption. According to the study by Reimers and Keast,⁴¹ tomato uptake by a typical consumer in the United States is 0.31 cups (\sim 40 g) a day. Considering that each person consumes between 3 and 5 pounds of food a day, the average tomato consumption is 1.7–2.9% of the total daily amount. On the basis of this, we chose 5% as the food amount slightly above the average of human consumption. The experiment was continued for 6 months. Prior to beginning the feeding regimen, as well as 1 and 3 months thereafter, blood samples (200 μ L) were collected via retro-orbital puncture under isoflurane anesthesia to monitor toxicity. Six months from the beginning of the experiment, the mice were euthanized, and blood and tissue were collected. Tissues were snap-frozen in liquid nitrogen or fixed in 10% buffered formalin and processed to determine CNT distribution by histology. Blood chemistry markers were measured to determine organ toxicity.

Blood Functional Toxicity Tests. Toxicity was assessed by measuring 14 blood markers of various organ functions as parts of the Comprehensive Diagnosis Kit (Abaxis, Union City, CA) and using the VetScan VS2 instrument (Abaxis). The organ injury markers included the following: alanine aminotransferase (ALT), albumin (ALB), alkaline phosphatase (ALP), amylase (AMY), blood urea nitrogen (BUN), calcium (CA), creatinine (CRE), globulin (GLOB), glucose (GLU), phosphorus (PHOS), potassium (K^+), sodium (Na^+), total bilirubin (TBIL), and total protein (TP). Our criteria for toxicity were the combination of (a) a statistically significant difference from the untreated and vehicle (water) controls, (b) going beyond normal lower and upper ranges, (c) dose dependence of the toxic response, if any, and (d) consistency between several functional markers of the same organ.

TUNEL Assay. Liver samples were embedded in paraffin, and 5- μ m sections were prepared. A TUNEL assay was performed and quantified as previously described.²⁵ Briefly, the samples were stained using the *In Situ* Cell Death Detection Kit (Roche Diagnostics, Indianapolis, IN) according to the manufacturer's protocol. After staining, cells were counterstained with 4',6-diamidino-2-phenylindol (DAPI) to visualize cell nuclei, mounted under coverslips with a Prolong Antifade kit (Invitrogen, Carlsbad, CA), and acquired using an Olympus IX-81 inverted microscope (Olympus America, Center Valley, PA) equipped with a Hamamatsu ORCA-ER monochrome camera (Hamamatsu Photonics K.K., Hamamatsu City, Japan).

Dark-Field Microscopy. CNT intracellular distributions were visualized using an Olympus IX-81 inverted microscope equipped with a CytoViva enhanced dark-field condenser. A full-spectrum halogen light source (150 W), Fiber-Lite DC-950 (Dolan-Jener), was used to illuminate the specimens in dark-field mode.

Transmission Electron Microscopy (TEM). TEM was performed as previously described.^{27,42} Dehydration was done with a graded ethanol series and embedded in Araldite 502/Embed 812 resin (EMS, Hatfield, PA). Ultrathin sections were obtained with a Leica Ultracut 7 microtome (Buffalo Grove, IL) and imaged at 80 kV on an FEI Technai G2 TF20 transmission electron microscope. Images were acquired with an FEI Eagle 4kX USB Digital Camera.

Quantification of the Amounts of Absorbed CNT in Organs of Mice. Calibration Sample Preparation. The whole animal organs

were taken out of -80°C storage and freeze-dried for at least 72 h to remove the water from the organs. After freeze-drying, the organs were ground using a mortar and pestle. Separately, 3 mg of carboxylic (COOH) functionalized multiwalled carbon nanotubes were dispersed in 100 mL of water and tip sonicated in continuous mode for 5 min at an amplitude intensity of 30%. Appropriate volumes of CNT dispersion were then added to the fixed amounts (20–30 mg) of control organ powder to obtain CNT loadings in the range of 0–50 $\mu\text{g/g}$. The calibration samples were freeze-dried again to remove any water from the CNT dispersion.

RF Heating of Animal Organs. Radio frequencies in the range of 1–300 MHz can also be used to induce heating in the samples and detect the presence of CNTs that rapidly heat up in response to RF. The flexibility to use various high electrical field intensity applicators make it simple and easier to use RF compared to microwaves, especially for complex matrices such as animal organs. A fringing-field applicator was used to induce RF heating in the powdered samples using a frequency of 138 MHz and power of 20 W. Both the dried calibration samples and the freeze-dried samples from all of the diets were transferred to a thin plastic boat and placed on the fringing-field applicator. It was made sure that the sample was confined between the two copper electrodes of the applicator such that the areal densities were in the range of 10–12 mg/cm^2 . A thermal camera (FLIR systems) was used to measure the maximum temperature observed over time (Figure S9). The heating rate was calculated for the initial 1 s of heating. A total of six measurements were taken, and the last three were used to calculate the average. Error bars were computed from differences between samples; note that diet A and diet B samples were combined to get a homogeneous baseline. After testing, the samples were stored under a vacuum at room temperature.

Limit of Detection. Calibration data were used to calculate the LOD. Linear regression was performed on the calibration data points, and the slope, m , of the line was determined. Standard error of the estimate, $s_{y/x}$, of temperature difference or heat rate (y) and the CNT content (x) was then calculated using eq 1.

$$s_{y/x} = \sqrt{\frac{\sum (y - y')^2}{n}} \quad (1)$$

where y is the temperature difference or heat rate measured using MIH or RF, respectively, y' is the temperature difference or heat rate predicted via regression line at the same CNT content, and n is the number of data points.

Limit of detection for temperature difference or heat rate, LOD_y , is given by eq 2.

$$\text{LOD}_y = k \cdot s_{y/x} \quad (2)$$

where the constant k is an expansion factor estimated by choosing the probability of false positive and negative errors to be 5% ($k = 3.3$ for plant calibration) or 10% ($k = 2.4$ for animal calibration).

The CNT content detection limit, LOD_x , was then calculated using eq 3.

$$\text{LOD}_x = \frac{\text{LOD}_y}{m} = \frac{k \cdot s_{y/x}}{m} \quad (3)$$

ASSOCIATED CONTENT

SI Supporting Information

The Supporting Information is available free of charge at <https://pubs.acs.org/doi/10.1021/acsnano.2c02201>.

Methods and materials for plant metabolite extraction and preparation for LC-MS, HPLC of tomatine, MIH calibration curve, schematic of setup to scan plant organs, thermal maps of root samples grown with and without CNTs, fold change analysis of all plant organs, top 10 metabolic pathways affected in tomato organs, association between TUNEL-positive liver cell nuclei and dark-field positive objects, calibration curve relating

heat rate with the CNT content in the liver, toxicity assessment of CNT-contaminated tomato fruits, schematic of the RF fringing-field applicator, estimation of the presence of CNT inside animal organs fed with tomato fruits (Figures S1–S10); total number of identified metabolites by KEGG, list of downregulated and upregulated metabolites in different tomato plant organs, list of pathways affected by dysregulated metabolites in tomato plant organs exposed to CNT (Tables S1–S11); characterization of CNT in different media during cultivation of plants exposed to CNT (Table S12) ([PDF](#))

AUTHOR INFORMATION

Corresponding Author

Mariya V. Khodakovskaya — Department of Biology, University of Arkansas at Little Rock, Little Rock, Arkansas 72204, United States;  orcid.org/0000-0001-6398-4105; Email: mvkhodakovsk@ualr.edu

Authors

Sajedeh Rezaei Cherati — Department of Biology, University of Arkansas at Little Rock, Little Rock, Arkansas 72204, United States;  orcid.org/0000-0002-7354-5293

Muhammad Anas — Artie McFerrin Department of Chemical Engineering, Texas A&M University, College Station, Texas 77843, United States

Shijie Liu — Department of Pharmacology and Toxicology, University of Arkansas for Medical Sciences, Little Rock, Arkansas 72205, United States

Sudha Shanmugam — Department of Biology, University of Arkansas at Little Rock, Little Rock, Arkansas 72204, United States;  orcid.org/0000-0002-3367-9772

Kamal Pandey — Department of Biology, University of Arkansas at Little Rock, Little Rock, Arkansas 72204, United States

Steven Angtuaco — Department of Pharmacology and Toxicology, University of Arkansas for Medical Sciences, Little Rock, Arkansas 72205, United States

Randal Shelton — Department of Pharmacology and Toxicology, University of Arkansas for Medical Sciences, Little Rock, Arkansas 72205, United States

Aida N. Khalfaoui — Artie McFerrin Department of Chemical Engineering, Texas A&M University, College Station, Texas 77843, United States

Savenka V. Alena — Department of Pharmacology and Toxicology, University of Arkansas for Medical Sciences, Little Rock, Arkansas 72205, United States

Erin Porter — Artie McFerrin Department of Chemical Engineering, Texas A&M University, College Station, Texas 77843, United States

Todd Fite — Central Arkansas Veterans Healthcare System, Little Rock, Arkansas 72207, United States

Huaixuan Cao — Artie McFerrin Department of Chemical Engineering, Texas A&M University, College Station, Texas 77843, United States

Micah J. Green — Artie McFerrin Department of Chemical Engineering, Texas A&M University, College Station, Texas 77843, United States;  orcid.org/0000-0001-5691-0861

Alexei G. Basnakian — Department of Pharmacology and Toxicology, University of Arkansas for Medical Sciences, Little Rock, Arkansas 72205, United States; Central Arkansas

Veterans Healthcare System, Little Rock, Arkansas 72207, United States

Complete contact information is available at:
<https://pubs.acs.org/10.1021/acsnano.2c02201>

Author Contributions

M.V.K. initiated the project. M.V.K., A.G.B., and M.J.G. designed metabolomics and toxicological and detection studies, supervised research, and wrote the manuscript. S.R C., S.S., and K.P. performed hydroponics studies and analysis of the total tomato metabolome. M.A., A.N.K., and E.P. performed studies on the detection of CNTs inside plant and animal organs. S.L., S.A., S.S., S.V.A., R.S., and T.F. performed *in vivo* and toxicological studies involving mice. H.C. performed characterization of carbon nanotubes in different mediums.

Notes

The authors declare no competing financial interest.

ACKNOWLEDGMENTS

This project was mainly supported by USDA-NIFA (AFRI Award 2017-07886 to M.V.K.). Toxicological work was partially supported by NIH grant 2P20 GM109005-06 and VA grant 2I01 BX002425 to A.G.B. The infrastructure for the metabolomics study was created using funds from NSF-EPSCoR grant 1826836 (Co-PI is M.V.K.).

REFERENCES

- (1) Sanzari, I.; Leone, A.; Ambrosone, A. Nanotechnology in Plant Science: To Make a Long Story Short. *Front. Bioeng. Biotechnol.* **2019**, *7*, DOI: 10.3389/fbioe.2019.00120.
- (2) Usman, M.; Farooq, M.; Wakeel, A.; Nawaz, A.; Cheema, S. A.; Rehman, H. ur; Ashraf, I.; Sanaullah, M. Nanotechnology in Agriculture: Current Status, Challenges and Future Opportunities. *Science of The Total Environment* **2020**, *721*, 137778.
- (3) Mittal, D.; Kaur, G.; Singh, P.; Yadav, K.; Ali, S. A. Nanoparticle-Based Sustainable Agriculture and Food Science: Recent Advances and Future Outlook. *Frontiers in Nanotechnology* **2020**, *2*, 10.
- (4) Shang, Y.; Hasan, M. K.; Ahammed, G. J.; Li, M.; Yin, H.; Zhou, J. Applications of Nanotechnology in Plant Growth and Crop Protection: A Review. *Molecules* **2019**, *24* (14), 2558.
- (5) *Plant Nanotechnology*, 1st ed.; Kole, C., Kumar, D. S., Khodakovskaya, M. V., Eds.; Springer International Publishing: Switzerland, 2016. DOI: 10.1007/978-3-319-42154-4.
- (6) He, X.; Deng, H.; Hwang, H. The Current Application of Nanotechnology in Food and Agriculture. *Journal of Food and Drug Analysis* **2019**, *27* (1), 1–21.
- (7) Khodakovskaya, M. V.; de Silva, K.; Nedosekin, D. A.; Dervishi, E.; Biris, A. S.; Shashkov, E. V.; Galanzha, E. I.; Zharov, V. P. Complex Genetic, Photothermal, and Photoacoustic Analysis of Nanoparticle-Plant Interactions. *Proc. Natl. Acad. Sci. U. S. A.* **2011**, *108* (3), 1028–1033.
- (8) Khodakovskaya, M. V.; Kim, B.-S.; Kim, J. N.; Alimohammadi, M.; Dervishi, E.; Mustafa, T.; Cerniglia, C. E. Carbon Nanotubes as Plant Growth Regulators: Effects on Tomato Growth, Reproductive System, and Soil Microbial Community. *Small* **2013**, *9* (1), 115–123.
- (9) Lahiani, M. H.; Dervishi, E.; Ivanov, I.; Chen, J.; Khodakovskaya, M. Comparative Study of Plant Responses to Carbon-Based Nanomaterials with Different Morphologies. *Nanotechnology* **2016**, *27* (26), 265102.
- (10) Lahiani, M. H.; Dervishi, E.; Chen, J.; Nima, Z.; Gaume, A.; Biris, A. S.; Khodakovskaya, M. V. Impact of Carbon Nanotube Exposure to Seeds of Valuable Crops. *ACS Appl. Mater. Interfaces* **2013**, *5* (16), 7965–7973.
- (11) Lahiani, M. H.; Chen, J.; Irin, F.; Puretzky, A. A.; Green, M. J.; Khodakovskaya, M. V. Interaction of Carbon Nanohorns with Plants: Uptake and Biological Effects. *Carbon* **2015**, *81*, 607–619.
- (12) Villagarcia, H.; Dervishi, E.; de Silva, K.; Biris, A. S.; Khodakovskaya, M. V. Bioreponse to Nanotubes: Surface Chemistry of Carbon Nanotubes Impacts the Growth and Expression of Water Channel Protein in Tomato Plants (Small 15/2012). *Small* **2012**, *8* (15), 2327.
- (13) Pandey, K.; Lahiani, M. H.; Hicks, V. K.; Hudson, M. K.; Green, M. J.; Khodakovskaya, M. Effects of Carbon-Based Nanomaterials on Seed Germination, Biomass Accumulation and Salt Stress Response of Bioenergy Crops. *PLoS One* **2018**, *13* (8), e0202274.
- (14) Pandey, K.; Anas, M.; Hicks, V. K.; Green, M. J.; Khodakovskaya, M. V. Improvement of Commercially Valuable Traits of Industrial Crops by Application of Carbon-Based Nanomaterials. *Sci. Rep.* **2019**, *9* (1), 19358.
- (15) Demirer, G. S.; Zhang, H.; Matos, J. L.; Goh, N. S.; Cunningham, F. J.; Sung, Y.; Chang, R.; Aditham, A. J.; Chio, L.; Cho, M.-J.; Staskawicz, B.; Landry, M. P. High Aspect Ratio Nanomaterials Enable Delivery of Functional Genetic Material without DNA Integration in Mature Plants. *Nat. Nanotechnol.* **2019**, *14* (5), 456–464.
- (16) Giraldo, J. P.; Landry, M. P.; Faltermeier, S. M.; McNicholas, T. P.; Iverson, N. M.; Boghossian, A. A.; Reuel, N. F.; Hilmer, A. J.; Sen, F.; Brew, J. A.; Strano, M. S. Plant Nanobionics Approach to Augment Photosynthesis and Biochemical Sensing. *Nat. Mater.* **2014**, *13* (4), 400–408.
- (17) Giraldo, J. P.; Wu, H.; Newkirk, G. M.; Kruss, S. Nanobiotechnology Approaches for Engineering Smart Plant Sensors. *Nat. Nanotechnol.* **2019**, *14* (6), 541–553.
- (18) McGehee, D. L.; Lahiani, M. H.; Irin, F.; Green, M. J.; Khodakovskaya, M. V. Multiwalled Carbon Nanotubes Dramatically Affect the Fruit Metabolome of Exposed Tomato Plants. *ACS Appl. Mater. Interfaces* **2017**, *9* (38), 32430–32435.
- (19) Irin, F.; Shrestha, B.; Cañas, J. E.; Saed, M. A.; Green, M. J. Detection of Carbon Nanotubes in Biological Samples through Microwave-Induced Heating. *Carbon* **2012**, *50* (12), 4441–4449.
- (20) Vashisth, A.; Upama, S. T.; Anas, M.; Oh, J.-H.; Patil, N.; Green, M. J. Radio Frequency Heating and Material Processing Using Carbon Susceptors. *Nanoscale Adv.* **2021**, *3* (18), 5255–5264.
- (21) Sweeney, C. B.; Moran, A. G.; Gruener, J. T.; Strasser, A. M.; Pospisil, M. J.; Saed, M. A.; Green, M. J. Radio Frequency Heating of Carbon Nanotube Composite Materials. *ACS Appl. Mater. Interfaces* **2018**, *10* (32), 27252–27259.
- (22) Nakayasu, M.; Ohno, K.; Takamatsu, K.; Aoki, Y.; Yamazaki, S.; Takase, H.; Shoji, T.; Yazaki, K.; Sugiyama, A. Tomato Roots Secrete Tomatine to Modulate the Bacterial Assemblage of the Rhizosphere. *Plant Physiology* **2021**, *186* (1), 270–284.
- (23) Schrenk, D.; Bignami, M.; Bodin, L.; Chipman, J. K.; del Mazo, J.; Hogstrand, C.; Hoogenboom, L.; Leblanc, J.-C.; Nebbia, C. S.; Nielsen, E.; Ntzani, E.; Petersen, A.; Sand, S.; Schwerdtle, T.; Vleminckx, C.; Wallace, H.; Brimer, L.; Cottrill, B.; Dusemund, B.; Mulder, P.; Vollmer, G.; Binaglia, M.; Ramos Bordajandi, L.; Riolo, F.; Roldán-Torres, R.; Grasl-Kraupp, B. Risk Assessment of Glycoalkaloids in Feed and Food, in Particular in Potatoes and Potato-Derived Products. *EFSA Journal* **2020**, *18* (8), e06222.
- (24) Moore, C. L.; Savenka, A. V.; Basnakian, A. G. TUNEL Assay: A Powerful Tool for Kidney Injury Evaluation. *Int. J. Mol. Sci.* **2021**, *22* (1), 412.
- (25) Darzynkiewicz, Z.; Galkowski, D.; Zhao, H. Analysis of Apoptosis by Cytometry Using TUNEL Assay. *Methods* **2008**, *44* (3), 250–254.
- (26) Sahu, S. C.; Hayes, A. W. Toxicity of Nanomaterials Found in Human Environment: A Literature Review. *Toxicology Research and Application* **2017**, *1*, 239784731772635.
- (27) Yang, S.-T.; Wang, X.; Jia, G.; Gu, Y.; Wang, T.; Nie, H.; Ge, C.; Wang, H.; Liu, Y. Long-Term Accumulation and Low Toxicity of Single-Walled Carbon Nanotubes in Intravenously Exposed Mice. *Toxicol. Lett.* **2008**, *181* (3), 182–189.

(28) Ryman-Rasmussen, J. P.; Andersen, M. E.; Bonner, J. C. Fate and Effects of Carbon Nanotubes Following Inhalation. In *The Toxicology of Carbon Nanotubes*; Poland, C., Bonner, J., Donaldson, K., Duffin, R., Eds.; Cambridge University Press: Cambridge, 2012; pp 118–133. DOI: 10.1017/CBO9780511919893.007.

(29) Murray, A. R.; Kisin, E.; Leonard, S. S.; Young, S. H.; Kommineni, C.; Kagan, V. E.; Castranova, V.; Shvedova, A. A. Oxidative Stress and Inflammatory Response in Dermal Toxicity of Single-Walled Carbon Nanotubes. *Toxicology* **2009**, *257* (3), 161–171.

(30) Jacobsen, N. R.; Møller, P.; Clausen, P. A.; Saber, A. T.; Micheletti, C.; Jensen, K. A.; Wallin, H.; Vogel, U. Biodistribution of Carbon Nanotubes in Animal Models. *Basic Clin Pharmacol Toxicol* **2017**, *121*, 30–43.

(31) Wang, H.; Wang, J.; Deng, X.; Sun, H.; Shi, Z.; Gu, Z.; Liu, Y.; Zhao, Y. Biodistribution of Carbon Single-Wall Carbon Nanotubes in Mice. *J. Nanosci Nanotechnol* **2004**, *4* (8), 1019–1024.

(32) Yuan, X.; Zhang, X.; Sun, L.; Wei, Y.; Wei, X. Cellular Toxicity and Immunological Effects of Carbon-Based Nanomaterials. *Particle and Fibre Toxicology* **2019**, *16* (1), 18.

(33) Wils, R. S.; Jacobsen, N. R.; Vogel, U.; Roursgaard, M.; Møller, P. Inflammatory Response, Reactive Oxygen Species Production and DNA Damage in Mice After Intrapleural Exposure to Carbon Nanotubes. *Toxicol. Sci.* **2021**, *183* (1), 184–194.

(34) Schipper, M. L.; Nakayama-Ratchford, N.; Davis, C. R.; Kam, N. W. S.; Chu, P.; Liu, Z.; Sun, X.; Dai, H.; Gambhir, S. S. A Pilot Toxicology Study of Single-Walled Carbon Nanotubes in a Small Sample of Mice. *Nat. Nanotechnol.* **2008**, *3* (4), 216–221.

(35) Farshad, O.; Heidari, R.; Zamiri, M. J.; Retana-Márquez, S.; Khalili, M.; Ebrahimi, M.; Jamshidzadeh, A.; Ommati, M. M. Spermatotoxic Effects of Single-Walled and Multi-Walled Carbon Nanotubes on Male Mice. *Frontiers in Veterinary Science* **2020**, *7*, 1007.

(36) Lahiani, M. H.; Khare, S.; Cerniglia, C. E.; Boy, R.; Ivanov, I. N.; Khodakovskaya, M. The Impact of Tomato Fruits Containing Multi-Walled Carbon Nanotube Residues on Human Intestinal Epithelial Cell Barrier Function and Intestinal Microbiome Composition. *Nanoscale* **2019**, *11* (8), 3639–3655.

(37) Lahiani, M. H.; Gokulan, K.; Williams, K.; Khodakovskaya, M. V.; Khare, S. Graphene and Carbon Nanotubes Activate Different Cell Surface Receptors on Macrophages before and after Deactivation of Endotoxins. *J. Appl. Toxicol.* **2017**, *37* (11), 1305–1316.

(38) Pluskal, T.; Castillo, S.; Villar-Briones, A.; Oresic, M. MZmine 2: Modular Framework for Processing, Visualizing, and Analyzing Mass Spectrometry-Based Molecular Profile Data. *BMC Bioinformatics* **2010**, *11*, 395.

(39) Ogata, H.; Goto, S.; Sato, K.; Fujibuchi, W.; Bono, H.; Kanehisa, M. KEGG: Kyoto Encyclopedia of Genes and Genomes. *Nucleic Acids Res.* **1999**, *27* (1), 29–34.

(40) Xia, J.; Sinelnikov, I. V.; Han, B.; Wishart, D. S. MetaboAnalyst 3.0—Making Metabolomics More Meaningful. *Nucleic Acids Res.* **2015**, *43* (W1), W251–257.

(41) Reimers, K. J.; Keast, D. R. Tomato Consumption in the United States and Its Relationship to the US Department of Agriculture Food Pattern: Results From What We Eat in America 2005–2010. *Nutrition Today* **2016**, *51* (4), 198–205.

(42) Pokrovskaya, I. D.; Joshi, S.; Tobin, M.; Desai, R.; Aronova, M. A.; Kamykowski, J. A.; Zhang, G.; Whiteheart, S. W.; Leapman, R. D.; Storrie, B. SNARE-Dependent Membrane Fusion Initiates α -Granule Matrix Decondensation in Mouse Platelets. *Blood Advances* **2018**, *2* (21), 2947–2958.

□ Recommended by ACS

Effects of Simulated Microgravity on the Internalization of Cerium Oxide Nanoparticles by Proliferating Human Skeletal Myoblasts

Giada Graziana Genchi, Gianni Ciofani, et al.

JUNE 02, 2023

ACS APPLIED NANO MATERIALS

READ ▶

Engineering Climate-Resilient Rice Using a Nanobiostimulant-Based “Stress Training” Strategy

Si Chen, Lijuan Zhao, et al.

MAY 31, 2023

ACS NANO

READ ▶

Intestinal Toxicity of Metal Nanoparticles: Silver Nanoparticles Disorder the Intestinal Immune Microenvironment

Quanzhong Ren, Rui Chen, et al.

JUNE 06, 2023

ACS APPLIED MATERIALS & INTERFACES

READ ▶

AgNPs-Triggered Seed Metabolic and Transcriptional Reprogramming Enhanced Rice Salt Tolerance and Blast Resistance

Xin Yan, Lijuan Zhao, et al.

DECEMBER 16, 2022

ACS NANO

READ ▶

Get More Suggestions >